Alexander Vogel, Jörg Nikolaus[a], Katrin Weise, Gemma Triola, Herbert Waldmann, Roland Winter, Andreas Herrmann and Daniel Huster*

Interaction of the human N-Ras protein with lipid raft model membranes of varying degrees of complexity

Abstract: Ternary lipid mixtures composed of cholesterol, saturated (frequently with sphingosine backbone), and unsaturated phospholipids show stable phase separation and are often used as model systems of lipid rafts. Yet, their ability to reproduce raft properties and function is still debated. We investigated the properties and functional aspects of three lipid raft model systems of varying degrees of biological relevance – PSM/POPC/Chol, DPPC/POPC/Chol, and DPPC/DOPC/Chol – using ^{2}H solid-state nuclear magnetic resonance (NMR) spectroscopy, fluorescence microscopy, and atomic force microscopy. While some minor differences were observed, the general behavior and properties of all three model mixtures were similar to previously investigated influenza envelope lipid membranes, which closely mimic the lipid composition of biological membranes. For the investigation of the functional aspects, we employed the human N-Ras protein, which is posttranslationally modified by two lipid modifications that anchor the protein to the membrane. It was previously shown that N-Ras preferentially resides in liquid-disordered domains and exhibits a time-dependent accumulation in the domain boundaries of influenza envelope lipid membranes. For all three model mixtures, we observed the same membrane partitioning behavior for N-Ras. Therefore, we conclude that even relatively simple models of raft membranes are able to reproduce many of their specific properties and functions.

Keywords: ^{2}H NMR; atomic force microscopy (AFM); confocal fluorescence microscopy lipid modification; membrane protein; order parameter.

[a]Present address: Yale University, 850 West Campus Dr., New Haven, CT 06516, USA.
*Corresponding author: Daniel Huster, Institute of Medical Physics and Biophysics, University of Leipzig, Härtelstraße 16-18, D-04107 Leipzig, Germany; and Tata Institute of Fundamental Research, Department of Chemical Sciences, Homi Bhabha Road, Colaba, Mumbai 400 005, India, e-mail: daniel.huster@medizin.uni-leipzig.de
Alexander Vogel: Institute of Medical Physics and Biophysics, University of Leipzig, Härtelstraße 16-18, D-04107 Leipzig, Germany

Jörg Nikolaus and Andreas Herrmann: Institute of Biology/Biophysics, Humboldt University Berlin, Invalidenstr. 43, D-10115 Berlin, Germany
Katrin Weise and Roland Winter: Physical Chemistry I, TU Dortmund University, Otto-Hahn-Str. 6, D-44227 Dortmund, Germany
Gemma Triola and Herbert Waldmann: Max Planck Institute of Molecular Physiology, Otto-Hahn-Str. 11, D-44227 Dortmund, Germany

Introduction

The existence of individual phases in lipid/water mixtures (Luzzati and Husson, 1962) and cell membranes (Reinert and Steim, 1970) had already been described several years before Singer and Nicolson developed their model of biological membranes, which implies that lipids are distributed homogeneously (Singer and Nicolson, 1972). Shortly afterwards, it was also suggested that several lipid phases can coexist in membranes (Pagano et al., 1973; Stier and Sackmann, 1973; Petit and Edidin, 1974). Later it was proposed that domains with different properties exist in lipid membranes (Karnovsky et al., 1982) and the concept was further developed in subsequent decades (Simons and Vanmeer, 1988; Simons and Ikonen, 1997). One particular type of microdomain, containing high amounts of cholesterol (Chol) as well as phospholipids with saturated acyl chains and sphingosine backbones, has unique properties. The lipids in this liquid-ordered (l_o) phase are packed rather tightly and the order in the acyl chains of the lipids is very high, similar to the gel phase of a membrane (Brown and London, 2000; Polozov and Gawrisch, 2006). However, the lipids can undergo rapid rotational and lateral diffusion more similar to a membrane in a liquid-disordered (l_d) phase (Kusumi et al., 1986; Brown and London, 2000; Filippov et al., 2004; Polozov and Gawrisch, 2006).

In the context of biological membranes, the l_o phase domains are referred to as lipid rafts and until now details about their shape, size, and lifetime are still a subject of debate (Leslie, 2011). The current model of rafts depicts

them as very dynamic in nature with a small size and short lifetime (Pike, 2006). It has also been proposed that the presence of proteins induces rafts by attractive interactions to a particular lipid species (Viola et al., 1999; Caroni, 2001; McLaughlin et al., 2002; Janosi and Gorfe, 2010; Janosi et al., 2012).

As investigations on naturally occurring rafts are difficult because of their small size and short lifetime, the biophysical properties of the raft-like l_o and l_d phases have been characterized using many different model systems (Ipsen et al., 1987; Marsh, 2010). In particular, ternary lipid mixtures consisting of cholesterol, a saturated (often with sphingosine backbone), and an unsaturated glycerophospholipid were used to study the phase behavior of these model systems (de Almeida et al., 2003; Veatch et al., 2007a; Bartels et al., 2008; Bunge et al., 2008; Ionova et al., 2012; Scheidt et al., 2013). While these investigations provide crucial information on biophysical properties of the individual phases, the systems are rather artificial and fail to reproduce certain aspects of rafts, such as their heterogeneous composition, small size, or short lifetime. Furthermore, rafts are thought to facilitate and modulate protein-protein interactions by specific enrichment of proteins in raft domains, leading to higher local concentrations and thus enhanced efficiency in signaling. Particularly, palmitoylated proteins were assumed to preferentially partition into rafts because of saturated lipid modifications (Casey, 1995; Wang et al., 2001; Zacharias et al., 2002). Therefore, the question that arises is: how relevant are such simple artificial model raft membrane systems? Here, we address this issue by investigating model raft systems with increasing biological relevance and their interaction with the membrane-associated lipid modified N-Ras protein.

N-Ras is a small GTPase that functions as a molecular switch in signal transduction cascades responsible for cell proliferation, differentiation, and growth (Brunsveld et al., 2006, 2009), and in its oncogenic form is strongly implicated in the formation of ~30% of all human tumors (Wittinghofer and Waldmann, 2000). The posttranslationally acquired lipid modifications that bind N-Ras to membranes (Casey, 1995; Gorfe et al., 2004) have been shown to be highly flexible and are able to adapt to almost any membrane environment (Huster et al., 2003; Vogel et al., 2005, 2007, 2009, 2010; Reuther et al., 2006b). In addition, it was shown that the lipid anchor of N-Ras controls the fast and reversible distribution of the protein over various cellular membranes (Rocks et al., 2005). Based on the membrane interaction of H-Ras, a model was proposed that involves a nucleotide-dependent association of Ras with l_d and raft-like membrane domains (Prior et al., 2003). However, recently an alternative model was developed that suggests that signaling of Ras is regulated by the altered access and residence time in a specific membrane compartment (Peyker et al., 2005; Weise et al., 2009, 2011; Janosi et al., 2012). This model is also in agreement with the observation that human N-Ras is preferentially localized in l_d domains and accumulates in the l_o/l_d phase boundaries of domain forming model raft membranes, independent of nucleotide-loading (Janosch et al., 2004; Vogel et al., 2009; Weise et al., 2009).

In this study, the viability of different raft model systems regarding the localization of N-Ras has been investigated. This addresses the issue of whether the membrane interaction of N-Ras is universal in heterogeneous membranes and answers the question of whether relatively simple model systems can be used for studies of membrane anchored proteins. In addition, the results are also relevant for the function of N-Ras which is closely related to its membrane environment.

Our previous investigation on the phase behavior of N-Ras in heterogeneous membranes was conducted on a membrane that consisted of lipids extracted from influenza envelope membranes, which represent the complex lipid composition of biological membranes (Vogel et al., 2009). Phase coexistence was observed by ^{2}H solid-state NMR spectroscopy, confocal fluorescence microscopy, and atomic force microscopy (AFM). It was shown that N-Ras accumulated in the phase boundaries of l_o and l_d domains. Here, we extend these investigations to three model systems of varying degrees of biological relevance: (i) PSM/POPC/Chol, (ii) DPPC/POPC/Chol, and (iii) DPPC/DOPC/Chol. The first system should be closest to a natural raft forming membrane as it contains palmitoyl-sphingomyelin (PSM), which is known to be strongly associated with the l_o phase. The naturally occurring POPC (1-palmitoyl-2-oleoyl-*sn*-glycero-3-phosphocholine) is enriched in the l_d phase. In the second system, PSM was replaced by (1,2-dipalmitoyl-*sn*-glycero-3-phosphocholine) – a simple disaturated lipid with a high phase transition temperature, which is also enriched in rafts. Finally, the more natural POPC was replaced by the artificial lipid DOPC (1,2-dioleoyl-*sn*-glycero-3-phosphocholine), which has a higher degree of unsaturation and a higher affinity for the l_d phase.

While minor differences were observed, the general behavior of N-Ras in all raft model systems was the same as in the viral membranes. In all systems, N-Ras was found to be distributed in the l_d phase but particularly accumulated at the phase boundary in a time-dependent manner, with very similar structure and dynamics of the lipid modifications of N-Ras. Therefore, even the relatively simple model

raft membrane systems are able to reproduce the complex behavior of membrane-associated proteins.

Results

The semisynthetic N-Ras protein used in this study consists of a G-domain and the hypervariable region comprising a linker domain and the posttranslationally modified C-terminal sequence that acts as the membrane anchor of N-Ras (Reuther et al., 2006a; Brunsveld et al., 2009). The posttranslational modifications are represented by a farnesyl (Far) and a hexadecyl (HD) chain that are attached to Cys 186 and 181, respectively, where the HD moiety is a nonhydrolyzable analog of the naturally occurring palmitoyl chain. ^{2}H solid-state NMR was used to investigate the structure and dynamics of the lipid chains of Ras and the lipids in the surrounding membrane mixtures. For each raft model membrane system, three samples were prepared: one sample in which the hexadecyl chain of N-Ras was perdeuterated and two samples in which either the phospholipid selective for the l_d or the l_o phase

was perdeuterated enabling the separate investigation of these lipid phases. We conducted ^{2}H solid-state NMR investigations on PSM/POPC/Chol and DPPC/POPC/Chol (molar ratio 38.5/38.5/23.1 in each system) in the presence of Ras. The temperature was set to 21.3°C as fluorescence microscopy showed only very little domain formation at 30°C, which was used for the other mixtures. Analysis of the DPPC/DOPC/Chol mixture (molar ratio 50/25/25) was not possible by NMR because DOPC is not available in the deuterated form.

The ^{2}H NMR spectra for the individual membrane components are plotted in Figure 1 and show only minor differences between the membrane mixtures. The saturated lipids PSM and DPPC, which are enriched in the l_o phase, exhibit very similar spectra although chemically they differ significantly. In all mixtures, the monounsaturated POPC was used as marker for the l_d phase and the spectrum is always narrower than that of the saturated lipid indicating lower order as expected for the l_d phase. The ^{2}H NMR spectra of POPC look very similar in the virus lipid (Vogel et al., 2009) and DPPC/POPC/Chol/Ras membranes but the spectrum in PSM/POPC/Chol/Ras membrane has a different shape. At its widest point, it is only slightly
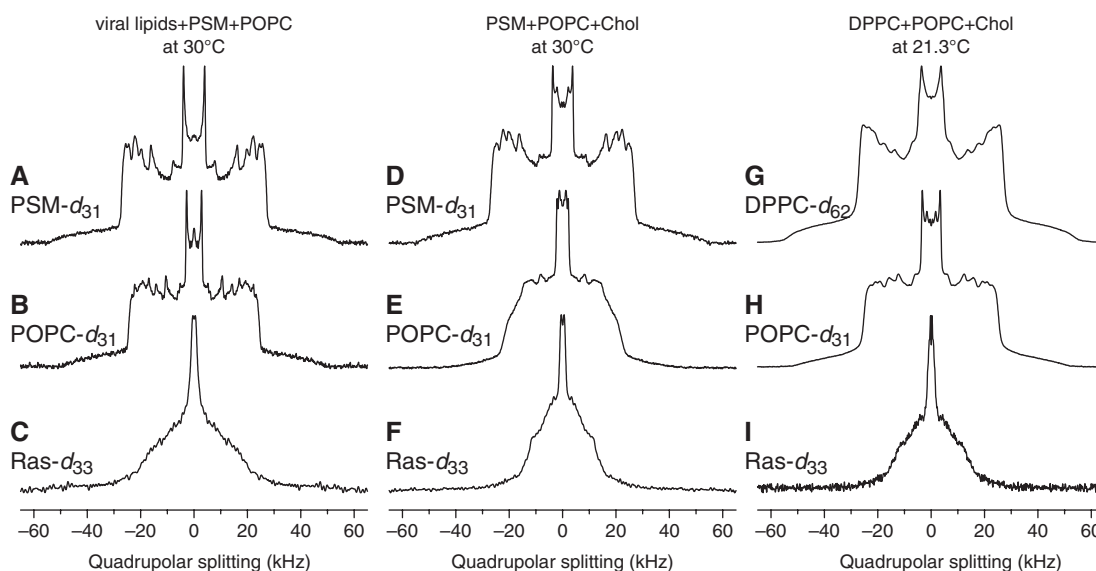

Figure 1 ^{2}H NMR spectra of the virus lipid membrane and two different raft model systems in the presence of N-Ras (molar ratio lipids/N-Ras 150/1).

Each depicted ^{2}H NMR spectrum comes from an individually labeled component of the ternary mixture. In the top row, the ^{2}H NMR spectra of the high melting lipid components are shown; in the middle row the ^{2}H NMR spectra of the POPC-d_{31} in the mixture are shown; and in the bottom row the ^{2}H NMR spectra of the deuterated N-Ras protein are shown. In membranes consisting of virus lipids/PSM/POPC (molar ratio 83.3/8.3/8.3) spectra of PSM-d_{31} (A), POPC-d_{31} (B), and the full-length N-Ras-d_{33} protein (C) were recorded at 30°C. In the PSM/POPC/Chol (molar ratio 38.5/38.5/23.1) mixture spectra of PSM-d_{31} (D), POPC-d_{31} (E), and the full-length N-Ras-d_{33} protein (F) were measured at 30°C while for the DPPC/POPC/Chol (molar ratio 38.5/38.5/23.1) mixture spectra of DPPC-d_{62} (G), POPC-d_{31} (H), and the full-length N-Ras-d_{33} protein (I) were measured at 21.3°C. The general shape of the spectra of the saturated (A, D, G) and unsaturated (B, E, H) lipid species as well as of the full-length N-Ras protein is very similar in the different membrane systems. Data for the virus lipids adopted from (Vogel et al., 2009).

Table 1 Summary of the quadrupolar splittings observed for the methyl groups of the two lipid components in the ²H NMR spectra of the raft mixtures.

	PSM/POPC/Chol		DPPC/POPC/Chol	
	PSM-d_{31}	POPC-d_{31}	DPPC-d_{62}	POPC-d_{31}
Quadrupolar splitting $\Delta\nu_Q^{small}$ /Hz	4510	2760	7700	3570
Quadrupolar splitting $\Delta\nu_Q^{large}$ /Hz	7700	4400	9390	6980

The values were obtained by fitting the spectrum.

narrower than in the other mixtures but its spectral shape has the appearance that a second even narrower spectrum is overlapping. Furthermore, the ²H NMR spectra of PSM, DPPC, and POPC in the PSM/POPC/Chol and DPPC/POPC/Chol mixtures but not the virus lipid membrane show two splittings for the smallest Pake-Doublet, which originates from the terminal methyl group of the acyl chain. In the ²H NMR spectrum of DPPC in the DPPC/POPC/Chol mixture, the second splitting is not as apparent but a small shoulder on the outer side of the methyl peak is visible, and by fitting all spectra the values of the quadrupolar splitting were determined (Table 1). The comparison shows that

the splitting of the saturated component (PSM or DPPC) and the splitting of the unsaturated component (POPC) are similar in both PSM/POPC/Chol and DPPC/POPC/Chol. Another remarkable observation is the shape of the spectra of the Ras lipid modifications, which are narrower, show poor spectral resolution, and do not resemble that of either of the lipids in all raft model systems.

To analyze the ²H NMR spectra quantitatively, smoothed chain order parameter plots were calculated providing the absolute order parameters $|S_{CD}^{(i)}|$ for each carbon segment of the deuterated palmitoyl chains in the lipids or the hexadecyl chain of the N-Ras protein as shown in Figure 2 (A, C, and E). The order parameter is a measure of the amplitude of motion of the individual carbon segment and therefore closely related to its dynamics. Overall, the agreement between the different membrane mixtures is very good. The saturated DPPC and PSM lipids have very similar order parameters, which are always significantly higher than those of the unsaturated POPC. Again, POPC has lower order in the PSM/POPC/Chol/Ras than in the other mixtures, which is a direct result of the apparent two overlapping components of the spectrum, one of which is very narrow. As expected from the even narrower spectra of the Ras lipid modifications
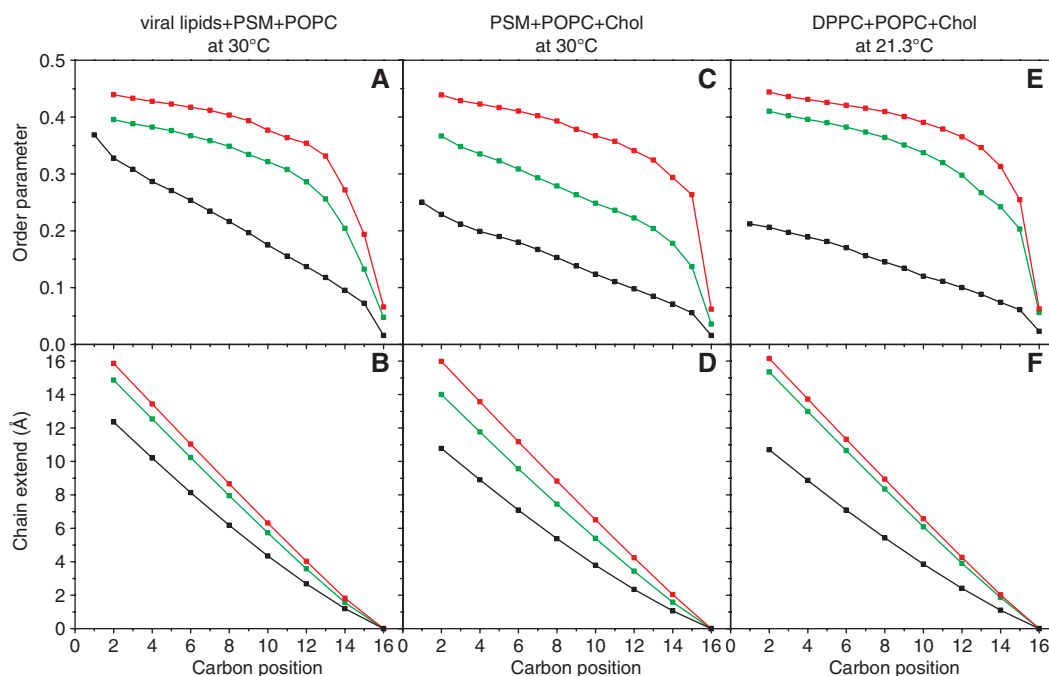

Figure 2 Order parameter profiles (A, C, E) and chain extension plots (B, D, F) of the virus lipid membrane lipids/PSM/POPC (molar ratio 83.3/8.3/8.3) (A, B) and two different raft model systems PSM/POPC/Chol (molar ratio 38.5/38.5/23.1) (C, D) and DPPC/POPC/Chol (molar ratio 38.5/38.5/23.1) (E, F) in the presence of N-Ras (molar ratio lipids/N-Ras 150/1).
Data obtained for PSM/DPPC are shown in red, while data for POPC are shown in green and data obtained for the full-length N-Ras protein are shown in black. In the raft model systems, the same general trends for the individual molecular species are observed as in the virus lipid membrane. Data for the virus lipids adopted from (Vogel et al., 2009).

their order parameters are much lower than those of the surrounding lipids.

From the order parameter profiles, detailed information about the geometry of the hydrocarbon chains can be extracted using a model describing the distribution of the orientations of the carbon segments (Petrache et al., 2000; Vogel et al., 2005). Values accessible by this model include chain length, interfacial area per chain, and hydrophobic thickness of the bilayer. In Figure 2 (B, D, and E), the chain extension plots calculated from the order parameter profiles are shown. These plots contain information about the mean position of every second carbon segment along the membrane normal, where the position of the terminal methyl group was set to zero for direct comparison. For all mixtures a mismatch between the saturated and the unsaturated lipid component is observed, which is on the order of ~1°Å in the virus lipid membranes and DPPC/POPC/Chol/Ras and ~2°Å in PSM/POPC/Chol/Ras. The Ras lipid modifications are always much shorter on average than the lipid acyl chains in both the l_o and l_d phase.

To investigate the distribution of the human N-Ras protein in these mixtures and also in DPPC/DOPC/Chol, giant unilamellar vesicles (GUVs) of all lipid mixtures were prepared and confocal laser scanning microscopy was conducted. The l_d phase was labeled with N-Rh-DOPE (red fluorescence) at a very low concentration of 0.2 mol%, which should not interfere with membrane domain formation (Veatch et al., 2007b). The results indicate the

coexistence of l_o and l_d domains at a broad temperature range (Figure 3, upper images). BODIPY-labeled N-Ras (green fluorescence) that was added to the GUVs yielding a 0.4 μm solution, is only localized in the l_d domains of all lipid mixtures (Figure 3). Furthermore, it is clearly visible that a significant portion of N-Ras is localized in the l_o/l_d phase boundary of these membranes (Figure 3, middle images). However, the marker for the l_d phase is not enriched in the phase boundary region. Fluorescence intensity profiles of the lower images emphasizing the preferred localization of BODIPY-N-Ras at the l_o/l_d phase boundary (green fluorescence) are also shown (Figure 3 lower images). The images of the virus lipid membranes were recorded at 4°C and 20°C while all other images were recorded at 25°C.

AFM was used to further visualize the distribution of lipid phases and the human N-Ras protein in the different membrane systems on the nanometer length scale. The different properties of the l_o and l_d phases lead to different thicknesses of the membrane domains detectable by AFM. The resulting AFM images of the partitioning of the Ras protein into the individual model membranes depicting the whole scan area before and after addition of N-Ras are given in Figure 4. Unfortunately, membranes consisting of DPPC/POPC/Chol did not show stable phase coexistence at room temperature and could not be investigated. The AFM images of the other membrane mixtures indicate phase separation in the absence of Ras, with varying
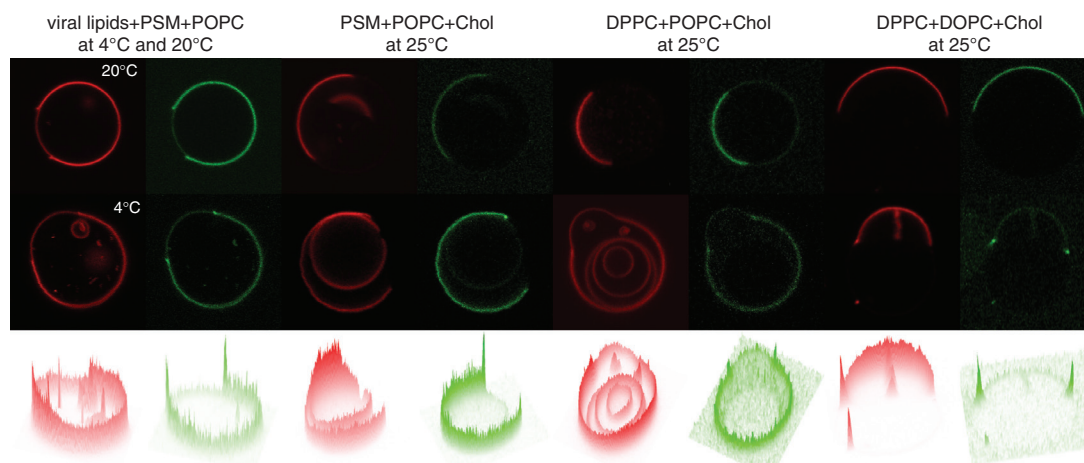

Figure 3 Confocal laser scanning microscopy images of GUVs incubated with 0.4 μm BODIPY-labeled N-Ras protein (green fluorescence). All membranes contained 0.2 mol% N-Rh-DOPE (red fluorescence), which enriches and therefore labels the l_d phase of the raft mixtures. The GUVs were composed of virus lipids/PSM/POPC/N-Rh-DOPE (molar ratio 83.2/8.3/8.3/0.2), PSM/POPC/Chol/N-Rh-DOPE (molar ratio 38.4/38.4/23.0/0.2), DPPC/POPC/Chol/N-Rh-DOPE (molar ratio 38.4/38.4/23.0/0.2), or DPPC/DOPC/Chol/N-Rh-DOPE (molar ratio 49.9/24.95/24.95/0.2). In all mixtures, the N-Ras proteins are localized in the l_d phase (upper images) and particularly at the l_o/l_d phase boundary (middle images). Fluorescence intensity profiles of the middle images emphasizing the preferred localization of BODIPY-N-Ras at the l_o/l_d phase boundary (green fluorescence) are shown below the fluorescence images. Data for the virus lipids adopted from (Vogel et al., 2009).
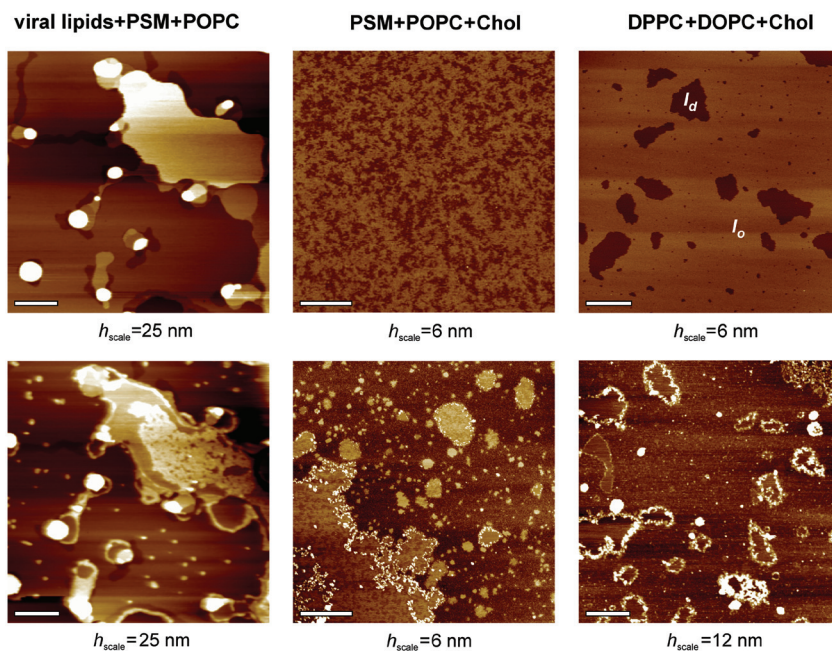
Figure 4 AFM images of lipid bilayers before (upper images) and after (lower images) addition of N-Ras.
The membranes were composed of either virus lipids/PSM/POPC (molar ratio 83.3/8.3/8.3), PSM/POPC/Chol (molar ratio 38.5/38.5/23.1), or DPPC/DOPC/Chol (molar ratio 50/25/25). All measurements were conducted at room temperature. The scale bar corresponds to 1 μm and the overall height of the vertical color scale h_{scale} is given below each image. AFM images are shown at characteristic time points of the time-dependent membrane partitioning process of N-Ras, with $t \approx 46$ h for all lower images. In all model membrane systems, a pronounced incorporation of N-Ras in the domain boundaries is detected, but the protein is also found in l_d domains while it is excluded from l_o domains. Data for the virus lipids adopted from (Vogel et al., 2009).

domain sizes. Upon addition of N-Ras to membranes consisting of PSM/POPC/Chol and DPPC/DOPC/Chol, the lateral organization of the membrane was changed by an increase in the amount of l_d phase. In addition, the incorporation of N-Ras nearly exclusively into the l_d phase of the membrane leads to a thinning of this fluid phase, as visible by an increased height difference with respect to the l_o phase. Whereas the N-Ras protein initially partitions into l_d domains of heterogeneous membranes, time-dependent diffusion and subsequent clustering of the protein in the l_o/l_d phase boundary region was observed for both systems, in line with previous studies (Vogel et al., 2009; Weise et al., 2009). This leads to a decrease of the unfavorable line tension between domains, which is also reflected in the fact that the l_o/l_d phase coexistence detected at the beginning of the AFM experiment, is abolished by the accumulation of N-Ras in the phase boundary region. As the clustering in the interfacial region of the domains is enhanced over time and the size of the protein particles located in the bulk l_d phase remains nearly constant over time, we speculate that clustering takes place mainly in the interfacial region. However, in the N-Ras GTP-loaded state some extent of clustering was also detected in the bulk fluid phase (cf. Weise et al., 2009).

In contrast, the lateral organization of the viral lipid membranes was not influenced by incubation of the membrane with N-Ras (Vogel et al., 2009). This could be explained the different mica-supported membranes: whereas one lipid bilayer was detected on the mica support for PSM/POPC/Chol and DPPC/DOPC/Chol, multiple lipid bilayers lying upon each other were observed for the viral membrane system. While the N-Ras membrane partitioning behavior is similar for all three membrane systems, model systems that more closely reflect the natural membrane showed a faster membrane partitioning and clustering of N-Ras (significant interfacial localization of N-Ras was detected after ~3 h for viral membranes and ~15 h for the other two systems). It is possible that these kinetic effects are related to a difference in the chain composition of the virus lipid membranes compared to the simpler model systems.

Discussion

We used three different model membrane systems (PSM/POPC/Chol, DPPC/POPC/Chol, and DPPC/DOPC/Chol) in

comparison to the previously studied virus lipid mix (Vogel et al., 2009) to investigate their viability as raft model systems and to evaluate whether the membrane partitioning of N-Ras depends on the membrane composition. The mixture containing 80 mol% virus lipids is the most natural system as it contained only 20 mol% of synthetic lipids (10 mol% PSM and 10 mol% POPC) as NMR labels. The other three model systems are synthetic lipid mixtures containing one saturated lipid component (either PSM or DPPC), one unsaturated lipid component (either POPC or DOPC), and cholesterol. The NMR data show that the saturated DPPC or PSM lipids have high order parameters and extended chain lengths in all mixtures (the mixture DPPC/DOPC/Chol could not be investigated by NMR), indicating that they form a l_o phase while the monounsaturated POPC has lower order and shorter chain length, indicating that it forms the l_d phase as expected (Polozov and Gawrisch, 2006; Bunge et al., 2008; Ionova et al., 2012). Both confocal fluorescence microscopy and AFM also reveal phase separation in all investigated mixtures over a broad range of temperatures (data not shown).

However, the NMR data also show some differences in the behavior of the different mixtures. In the ^{2}H NMR spectra of the PSM/POPC/Chol and DPPC/POPC/Chol mixtures, a second component is detected, which suggests that the lipids are not purely localized in one phase each. Rather, monounsaturated lipids are also found in smaller concentration in the l_o phase and vice versa. Most interesting are the quadrupolar splittings for the terminal methyl groups of the individual lipid species, which are least influenced by the differences in the head groups of the lipids and therefore most indicative of the properties of the surrounding lipid phase. In fact, it was shown that PSM and POPC in a homogeneous 1:1 mixture exhibit very similar quadrupolar splittings (difference <200 Hz) for the terminal methyls (Bunge et al., 2008). In the virus lipid membrane, the difference between POPC and PSM is ~2200 Hz, which clearly indicates that both experience a different environment. In the PSM/POPC/Chol and DPPC/POPC/Chol mixtures, two splittings are observed for each lipid species. Comparison of the spectra reveals that one splitting of the saturated lipid (PSM or DPPC) and one splitting of POPC are almost identical in both membrane systems, which also was observed in other studies (Bartels et al., 2008). This indicates that both lipid species spend a considerable amount of time in a common environment. In addition to the common quadrupolar splitting, the saturated lipids (PSM or DPPC) exhibit a second spectral component with a quadrupolar splitting, which is larger while the second splitting observed for POPC is smaller in both PSM/POPC/Chol and DPPC/POPC/Chol indicating that

both lipid species also spend time in environments separated from each other where the environment that POPC experiences is less ordered than the environment of DPPC and PSM. Analysis of the intensity of the peaks shows that in the PSM/POPC/Chol mixture the saturated and unsaturated lipids spend less time in the common environment than they do in the DPPC/POPC/Chol mixture. This indicates that the more time components of a mixture spend in a common environment, the more artificial the system is. As neither AFM nor confocal fluorescence imaging show such a common phase, these fluctuations have to be very small. One possibility is that the domain boundaries become wider and form this common phase. The molecular reason why DPPC/POPC/Chol exhibits more of this common phase than PSM/POPC/Chol, even though DPPC/POPC/Chol was investigated at lower temperature, might be due to the fact that cholesterol interacts more strongly with sphingomyelin than with DPPC (Oradd et al., 2005; Aittoniemi et al., 2007). This stronger interaction probably leads to higher cholesterol concentrations in the l_o and lower cholesterol concentrations in the l_d phase amplifying the difference in order between them promoting phase separation.

Unfortunately, it is not possible to estimate the amount of cholesterol in each phase from the ^{2}H NMR spectra because each phase will also contain lipids that favor the other phase and thereby also influence the order parameters. For instance, if phase separation of a PSM/POPC/Chol mixture (molar ratio 37.5/37.5/25) was complete and cholesterol would distribute evenly over both phases, the l_o phase would consist of PSM/Chol (molar ratio 37.5/12.5). A former study investigated these two systems and found that the order parameters of PSM in PSM/Chol (molar ratio 37.5/12.5) are much higher than those in PSM/POPC/Chol (molar ratio 37.5/37.5/25) (Bunge et al., 2008) indicating that POPC is present in the l_o phase of PSM/POPC/Chol. Furthermore, in this publication, the authors also measured the order parameters of POPC in the same mixture. Therefore, this publication represents a good comparison to our studies although the order parameters shown were acquired at 40°C. Yet, the relative difference between the order parameters of PSM and POPC in the PSM/POPC/Chol mixture (molar ratio 37.5/37.5/25) at 40°C is very close to the difference we observe between PSM and POPC in PSM/POPC/Chol (molar ratio 38.5/38.5/23.1) in the presence of N-Ras at 30°C. Therefore, we can conclude that at least for this mixture the presence of N-Ras does not lead to significant changes in the molecular composition of either the l_o or l_d phase.

In addition to these investigations on the state of the lipids, our assay also offers an assessment of the raft

model systems from a functional point of view. For this, we employed the human N-Ras protein, which was shown to be preferentially associated with the l_d phase and particularly accumulates in a time-dependent manner in the phase boundaries of the domains in virus lipids/PSM/POPC and DPPC/DOPC/Chol mixtures (Vogel et al., 2009; Weise et al., 2009). The same behavior is observed in all other raft model systems investigated. The ^{2}H NMR spectra of the Ras lipid are very narrow, show poor spectral resolution, and do not resemble that of either lipid component in all raft model systems. Such ^{2}H NMR spectra are indicative of slower motions with microsecond correlation times, similar to a critical behavior with significant fluctuations at the critical point of a ternary lipid mixture (Veatch et al., 2007a). The order parameters and chain lengths that were calculated from these spectra show that the length of the saturated Ras lipid modification varies depending on membrane composition. It is the longest and most ordered in the virus lipid membranes while it exhibits reduced order in PSM/POPC/Chol and DPPC/POPC/Chol. Furthermore, the spectra are superimposed with a small isotropic signal. Such phenomena are often encountered in biological membranes and can be explained by highly mobile lipid chains (Gamier-Lhomme et al., 2007), which would suggest that a small portion of the Ras chains is isotropically mobile and, very likely, not inserted into the membrane. Therefore, this spectral shape is interpreted such that N-Ras is located in the l_o/l_d phase boundaries, where a very heterogeneous environment is present, which leads to the observed effects on the spectrum (Vogel et al., 2009). Confocal fluorescence microscopy and AFM provide even more direct evidence for this hypothesis. In all mixtures, a time-dependent accumulation of N-Ras in the domain boundaries is clearly observed. Therefore, we conclude that the general behavior of N-Ras is the same in all mixtures, where it shows a clear preference for the l_d phase of the membrane and given enough time accumulates in the phase boundaries.

The accumulation of N-Ras in the domain boundaries is associated with the line tension of these boundaries (McConnell and Vrljic, 2003; Kuzmin et al., 2005; Vogel et al., 2009). The entropic penalty for association of proteins with the phase boundary might be countered by a reduction of its line tension. This is particularly interesting because this might be crucial for the function of N-Ras (Vogel et al., 2009). Assuming a homogenous membrane, the binding of proteins reduces the dimensionality of diffusion from 3 to 2 and thereby increases the likelihood to meet an interaction partner that is also bound at the membrane (Murray et al., 1997). However, this effect is countered by the difference in the diffusion coefficients

of proteins in cytosol ($D \approx 10^{-10}$ m^2/s) and in membranes ($D \approx 10^{-11}$–10^{-12} m^2/s) such that the overall contact probability remains relatively constant (Haugh and Lauffenburger, 1997). But if both interaction partners are co-localized in rafts or even their boundaries their accessible surface area is significantly reduced and their interaction efficiency is increased despite the lower diffusion coefficient in the membrane. In addition, the reduction of line tension by accumulation of lipidated proteins such as N-Ras in the interfacial region of heterogeneous membranes fosters self-association and cluster formation of N-Ras at the domain boundaries. From previous AFM experiments it was proposed that the bulky and branched farnesyl anchor is largely responsible for the interfacial membrane accumulation of N-Ras, as this membrane partitioning behavior was observed for several N-Ras lipidation motifs including at least one farnesyl anchor (Weise et al., 2009). Such an interfacial adsorption effect can generally be expected in many-phase lipid systems for inserting proteins that have no preference for any particular phase – for example because of hydrophobic mismatch and/or entropic reasons – so that the proteins are expelled to the boundary (Janosi et al., 2012; Li et al., 2012; Li and Gorfe, 2013). Furthermore, it was reported that N-Ras forms dimers in POPC membranes, which might be further promoted by an increase in the local concentration (Gueldenhaupt et al., 2012).

In conclusion, from the viewpoint of the distribution and general behavior of the human N-Ras protein, all lipid mixtures used in this study qualify as viable raft model systems. However, if details such as the length and order of the lipid modifications of Ras or the size and stability of the domains are investigated, one has to be careful about choosing a model system that is as close as possible to the native environment. In the best case, such lipid systems should be prepared from raft-prone natural membranes, such as caveolae, but the amounts that can be recovered from such systems are too small for many biophysical techniques.

Materials and methods

Materials

The lipids N-palmitoyl-D-*erythro*-sphingosylphosphorylcholine (PSM), N-perdeuteriopalmitoyl-D-*erythro*-sphingosylphosphorylcholine (PSM-d_{31}), 1,2-dipalmitoyl-*sn*-glycero-3-phosphocholine (DPPC), 1,2-diperdeuteriopalmitoyl-*sn*-glycero-3-phosphocholine (DPPC-d_{62}), 1-palmitoyl-2-oleoyl-*sn*-glycero-3-phosphocholine (POPC), 1-perdeuteriopalmitoyl-2-oleoyl-*sn*-glycero-3-phosphocholine (POPC-d_{31}),

1,2-dioleoyl-*sn*-glycero-3-phosphocholine (DOPC), and 1,2-dioleoyl-*sn*-glycero-3-phosphoethanolamine-N-(lissamine rhodamine B sulfonyl) (N-Rh-DOPE) as well as cholesterol (Chol) were procured from Avanti Polar Lipids, Inc. (Alabaster, AL, USA) and used without further purification. Virus lipids were extracted from influenza virus (strain A/PR/8/34). For all measurements the same lipid batches were used.

Protein synthesis

The N-Ras peptide with the sequence H-Gly-Cys(HD)-Met-Gly-Leu-Pro-Cys(Far)-OMe and perdeuterated hexadecyl (HD) chains as well as an N-terminal maleimidocaproyl-function was synthesized as before (Bader et al., 2000; Volkert et al., 2003). C-terminally truncated wildtype N-Ras (1-181) was expressed in *Escherichia coli* CK600K and purified via DEAE ion exchange chromatography and gel filtration. Coupling with N-Ras peptides was performed in stoichiometric amounts in 20 mM Tris, pH 7.4, 5 mM MgCl$_2$ supplemented with Triton X114. After removal of Triton by DEAE ion exchange chromatography, Ras was concentrated in 20 mM Tris, pH 7.4, 5 mM MgCl$_2$, 2 mM DTE by size exclusion filtration. Proteins were analyzed by SDS-PAGE and MALDI-TOF MS.

^{2}H NMR spectroscopy

Aliquots of the phospholipids were co-dissolved in chloroform, dried under vacuum (10 mbar), and dispersed in water. The suspension was vortexed for 10 min, incubated for 30 min at 37°C, shock frozen in liquid nitrogen and thawed 10 times. Large unilamellar vesicles were prepared by 10 cycles of extrusion across polycarbonate membranes with 100 nm pores. N-Ras protein was added to the liposomes at a protein to lipid molar ratio of 1:150. The suspension was ultracentrifuged, the pellet lyophilized and hydrated to 50wt% water. Samples were equilibrated, transferred to 5-mm glass vials, and sealed. ^{2}H NMR spectra were acquired on an Avance 750 NMR spectrometer. The spectra were accumulated with a spectral width of ±250 kHz, 3 μs π/2 pulses separated by a 60 μs delay, and a relaxation delay of 1 s.

Confocal laser scanning microscopy

Giant unilamellar vesicles (GUV) were prepared by electroformation (Angelova et al., 1992) containing 0.2 mol% N-Rh-DOPE as l_d phase marker in sucrose buffer. BODIPY-labeled N-Ras protein was added to GUVs yielding a 0.4 μM solution at 25°C. Confocal images of the equatorial plane of the GUVs were taken using an inverted confocal laser scanning microscope (FV1000, Olympus, Hamburg, Germany) using a 60× (N.A. 1.35) oil-immersion objective. Rhodamine and BODIPY were excited with a 559 nm diode laser and the 488 nm line of an Ar-ion laser (Olympus, Hamburg, Germany), respectively. The emissions of rhodamine and BODIPY were recorded between 570 nm and 670 nm and between 500 nm and 545 nm, respectively.

AFM

Supported lipid bilayers were produced of the dry lipid mixture hydrated with Tris buffer as described before (Weise et al., 2009, 2011; Vogel et al., 2009), but vesicle fusion was carried out at 70°C for DPPC/DOPC/Chol (molar ratio 50/25/25; 20 mM Tris, 5 mM MgCl$_2$, pH 7.4) and PSM/POPC/Chol (molar ratio 38.5/38.5/23.1; 20 mM Tris, 5 mM MgCl$_2$, pH 7.4) as well as 90°C for the viral lipid system (20 mM Tris, 7 mM MgCl$_2$, pH 7.4) (Weise et al., 2009). 200 μl of N-Ras in Tris buffer (100 μg/ml) were slowly injected into the AFM fluid cell at room temperature and incubated for 1 h. AFM measurements were performed on a MultiMode scanning probe microscope equipped with a NanoScope IIIa controller (Digital Instruments, Santa Barbara, CA, USA) and J-Scanner (scan size 125 μm). Images were obtained in tapping mode in liquid with sharp nitride lever (SNL) or oxide-sharpened silicon nitride (DNP-S) probes mounted in a fluid cell (MTFML, Veeco Instruments, Mannheim, Germany). Tips with nominal force constants of 0.32 N/m were used at driving frequencies around 9 kHz; scan frequencies were between 0.5 and 1.5 Hz. Height and phase images were acquired with resolutions of 512×512 pixels and image analysis and processing was carried out by use of software NanoScope version 5.

References

Aittoniemi, J., Niemela, P.S., Hyvonen, M.T, Karttunen, M., and Vattulainen, I. (2007). Insight into the putative specific interactions between cholesterol, sphingomyelin and palmitoyl-oleoyl phosphatidylcholine. Biophys. J. *92*, 1125–1137.

Angelova, M., Soléau, S., Méléard, P., Faucon, F., and Bothorel, P. (1992). Preparation of giant vesicles by external AC electric fields. Kinetics and applications. In: Trends in Colloid and Interface Science VI. C. Helm, M. Lösche and H. Möhwald, eds. (Berlin/Heidelberg: Springer), pp. 127–131.

Bader, B., Kuhn, K., Owen, D.J., Waldmann, H., Wittinghofer, A., and Kuhlmann, J. (2000). Bioorganic synthesis of lipid-modified proteins for the study of signal transduction. Nature *403*, 223–226.

Bartels, T., Lankalapalli, R.S., Bittman, R., Beyer, K., and Brown, M.F. (2008). Raftlike mixtures of sphingomyelin and cholesterol investigated by solid-state ^{2}H NMR spectroscopy. J. Am. Chem. Soc. *130*, 14521–14532.

Brown, D.A. and London, E. (2000). Structure and function of sphingolipid- and cholesterol-rich membrane rafts. J. Biol. Chem. *275*, 17221–17224.

Brunsveld, L., Kuhlmann, J., Alexandrov, K., Wittinghofer, A., Goody, R.S., and Waldmann, H.. (2006). Lipidated Ras and Rab peptides and proteins – synthesis, structure and function. Angew. Chem. Int. Ed. *45*, 6622–6646.

Brunsveld, L., Waldmann, H. and Huster, D. (2009). Membrane binding of lipidated Ras peptides and proteins – the structural point of view. Biochim. Biophys. Acta *1788*, 273–288.

Bunge, A., Müller, P., Stöckl, M., Herrmann, A., and Huster, D. (2008). Characterization of the Ternary Mixture of Sphingomyelin, POPC, and cholesterol: support for an inhomogeneous lipid distribution at high temperatures. Biophys. J. *94*, 2680–2690.

Caroni, P. (2001). Actin cytoskeleton regulation through modulation of PI(*4*, 5)P-2 rafts. EMBO J. *20*, 4332–4336.

Casey, P.J. (1995). Protein lipidation in cell signaling. Science *268*, 221–225.

de Almeida, R.F., M., Fedorov, A., and Prieto, M. (2003). Sphingomyelin/phosphatidylcholine/cholesterol phase diagram, boundaries and composition of lipid rafts. Biophys. J. *85*, 2406–2416.

Filippov, A., Oradd, G., and Lindblom, G. (2004). Lipid lateral diffusion in ordered and disordered phases in raft mixtures. Biophys. J. *86*, 891–896.

Gamier-Lhomme, M., Grelard, A., Byrne, R.D., Loudet, C., Dufourc, E.J., and Larijani, B. (2007). Probing the dynamics of intact cells and nuclear envelope precursor membrane vesicles by deuterium solid state NMR spectroscopy. Biochim. Biophys. Acta *1768*, 2516–2527.

Gorfe, A.A., Pellarin, R., and Caflisch, A. (2004). Membrane localization and flexibility of a lipidated ras peptide studied by molecular dynamics simulations. J. Am. Chem. Soc. *126*, 15277–15286.

Gueldenhaupt, J., Rudack, T., Bachler, P., Mann, D., Triola, G., Waldmann, H., Koetting, C., and Gerwert, K. (2012). N-Ras forms dimers at POPC membranes. Biophys. J. *103*, 1585–1593.

Haugh, J.M. and Lauffenburger, D.A. (1997). Physical modulation of intracellular signaling processes by locational regulation. Biophys. J. *72*, 2014–2031.

Huster, D., Vogel, A., Katzka, C., Scheidt, H.A., Binder, H., Dante, S., Gutberlet, T., Zschörnig, O., Waldmann, H., and Arnold, K. (2003). Membrane insertion of a lipidated Ras peptide studied by FTIR, solid-state NMR and neutron diffraction spectroscopy. J. Am. Chem. Soc. *125*, 4070–4079.

Ionova, I.V., Livshits, V.A., and Marsh, D. (2012). Phase diagram of ternary cholesterol/palmitoylsphingomyelin/palmitoyloleoyl-phosphatidylcholine mixtures, spin-label EPR study of lipid-raft formation. Biophys. J. *102*, 1856–1865.

Ipsen, J.H., Karlstrom, G., Mouritsen, O.G., Wennerstrom, H., and Zuckermann, M.J. (1987). Phase-equilibria in the phosphatidylcholine-cholesterol system. Biochim. Biophys. Acta *905*, 162–172.

Janosch, S., Nicolini, C., Ludolph, B., Peters, C., Volkert, M., Hazlet, T.L., Gratton, E., Waldmann, H., and Winter, R. (2004). Partitioning of dual-lipidated peptides into membrane microdomains, lipid sorting vs peptide aggregation. J. Am. Chem. Soc. *126*, 7496–7503.

Janosi, L. and Gorfe, A.A. (2010). Segregation of negatively charged phospholipids by the polycationic and farnesylated membrane anchor of Kras. Biophys. J. *99*, 3666–3674.

Janosi, L., Li, Z., Hancock, J.F., and Gorfe, A.A. (2012). Organization, dynamics and segregation of Ras nanoclusters in membrane domains. Proc. Natl. Acad. Sci. USA *109*, 8097–8102.

Karnovsky, M.J., Kleinfeld, A.M., Hoover, R.L., and Klausner, R.D. (1982). The concept of lipid domains in membranes. J. Cell Biol. *94*, 1–6.

Kusumi, A., Subczynski, W.K., Pasenkiewiczgierula, M., Hyde, J.S., and Merkle, H. (1986). Spin-label studies on phosphatidylcholine-cholesterol membranes – effects of alkyl chain-length and unsaturation in the fluid phase. Biochim. Biophys. Acta *854*, 307–317.

Kuzmin, P.I., Akimov, S.A., Chizmadzhev, Y.A., Zimmerberg, J., and Cohen, F.S. (2005). Line tension and interaction energies of membrane rafts calculated from lipid splay and tilt. Biophys. J. *88*, 1120–1133.

Leslie, M. (2011). Do lipid rafts exist? Science *334*, 1046–1047.

Li, Z. and Gorfe, A.A. (2013). Deformation of a two-domain lipid bilayer due to asymmetric insertion of lipid-modified Ras paptides. Soft Matter *9*, 11249–11256.

Li, Z., Janosi, L., and Gorfe, A.A. (2012). Formation and domain partitioning of H-ras peptide nanoclusters, effects of peptide concentration and lipid composition. J. Am. Chem. Soc. *134*, 17278–17285.

Luzzati, V. and Husson, F. (1962). The structure of the liquid-crystalline phases of lipid-water systems. J. Cell Biol. *12*, 207–219.

Marsh, D. (2010). Liquid-ordered phases induced by cholesterol: A compendium of binary phase diagrams. Biochim. Biophys. Acta Biomembr. *1798*, 688–699.

McConnell, H.M. and Vrljic, M. (2003). Liquid-liquid immiscibility in membranes. Annu. Rev. Biophys. Biomol. Struct. *32*, 469–492.

McLaughlin, S., Wang, J.Y., Gambhir, A., and Murray, D. (2002). PIP$_2$ and proteins, Interactions, organization and information flow. Annu. Rev. Biophys. Biomol. Struct. *31*, 151–175.

Murray, D., Ben-Tal, N., Honig, B., and McLaughlin, S. (1997). Electrostatic interaction of myristoylated proteins with membranes, simple physics, complicated biology. Structure *5*, 985–989.

Oradd, G., Westerman, P.W., and Lindblom, G. (2005). Lateral diffusion coefficients of separate lipid species in a ternary raft-forming bilayer, a Pfg-NMR multinuclear study. Biophys. J. *89*, 315–320.

Pagano, R.E., Cherry, R.J., and Chapman, D. (1973). Phase-transitions and heterogeneity in lipid bilayers. Science *181*, 557–559.

Petit, V.A. and Edidin, M. (1974). Lateral phase separation of lipids in plasma-membranes – Effect of temperature on mobility of membrane antigens. Science *184*, 1183–1185.

Petrache, H.I., Dodd, S.W., and Brown, M.F. (2000). Area per lipid and acyl length distributions in fluid phosphatidylcholines determined by ^{2}H NMR spectroscopy. Biophys. J. *79*, 3172–3192.

Peyker, A., Rocks, O., and Bastiaens, P.I.H. (2005). Imaging activation of two Ras isoforms simultaneously in a single cell. ChemBioChem *6*, 78–85.

Pike, L.J. (2006). Rafts defined, a report on the Keystone Symposium on Lipid Rafts and Cell Function. J. Lipid Res. *47*, 1597–1598.

Polozov, I.V. and Gawrisch, K. (2006). Characterization of the liquid-ordered state by proton MAS NMR. Biophys. J. *90*, 2051–2061.

Prior, I.A., Muncke, C., Parton, R.G., and Hancock, J.F. (2003). Direct visualization of Ras proteins in spatially distinct cell surface microdomains. J. Cell Biol. *160*, 165–170.

Reinert, J.C. and Steim, J.M. (1970). Calorimetric detection of a membrane-lipid phase transition in living cells. Science *168*, 1580–1582.

Reuther, G., Tan, K.T., Kohler, J., Nowak, C., Pampel, A., Arnold, K., Kuhlmann, J., Waldmann, H., and Huster, D. (2006a). Structural model of the membrane-bound C terminus of lipid-modified human N-ras protein. Angew. Chem. Int. Ed. *45*, 5387–5390.

Reuther, G., Tan, K.T., Vogel, A., Nowak, C., Arnold, K., Kuhlmann, J., Waldmann, H., and Huster, D. (2006b). The lipidated membrane anchor of full length N-Ras protein shows an extensive dynamics as revealed by solid-state NMR spectroscopy. J. Am. Chem. Soc. *128*, 13840–13846.

Rocks, O., Peyker, A., Kahms, M., Verveer, P.J., Koerner, C., Lumbierres, M., Kuhlmann, J., Waldmann H., Wittinghofer, A., and Bastiaens, P.I.H. (2005). An acylation cycle regulates localization and activity of palmitoylated Ras isoforms. Science *307*, 1746–1752.

Scheidt, H., A., Meyer, T., Nikolaus, J., Baek, D.J. Haralampiev, I., Thomas, L., Bittman, R., Müller, P., Herrmann, A., and Huster, D. Cholesterol's aliphatic side chain structure modulates membrane properties. (2013). Angew. Chem. Int. Ed. *52*, 12848–12851.

Simons, K. and Ikonen, E. (1997). Functional rafts in cell membranes. Nature *387*, 569–572.

Simons, K. and Vanmeer, G. (1988). Lipid sorting in epithelial cells. Biochemistry *27*, 6197–6202.

Singer, S.J. and Nicolson, G.L. (1972). Fluid mosaic model of structure of cell-membranes. Science *175*, 720–731.

Stier, A. and Sackmann, E. (1973). Spin labels as enzyme substrates, Heterogeneous lipid distribution in liver microsomal membranes. Biochim. Biophys. Acta, Biomembr. *311*, 400–408.

Veatch, S.L., Soubias, O., Keller, S.L., and Gawrisch, K. (2007a). Critical fluctuations in domain-forming lipid mixtures. Proc. Natl. Acad. Sci. USA *104*, 17650–17655.

Veatch, S.L., Leung, S.S.W., Hancock, R.E.W., and Thewalt, J.L. (2007b). Fluorescent probes alter miscibility phase boundaries in ternary vesicles. J. Phys. Chem. B. *111*, 502–504.

Viola, A., Schroeder, S., Sakakibara, Y., and Lanzavecchia, A. (1999). T lymphocyte costimulation mediated by reorganization of membrane microdomains. Science *283*, 680–682.

Vogel, A., Katzka, C.P., Waldmann, H., Arnold, K., Brown, M.F., and Huster, D. (2005). Lipid modifications of a Ras peptide exhibit altered packing and mobility versus host membrane as detected by ^{2}H solid-state NMR. J. Am. Chem. Soc. *127*, 12263–12272.

Vogel, A., Tan, K.T., Waldmann, H., Feller, S.E., Brown, M.F., and Huster, D. (2007). Flexibility of ras lipid modifications studied by ^{2}H solid-state NMR and molecular dynamics simulations. Biophys. J. *93*, 2697–2712.

Vogel, A., Reuther, G., Weise, K., Triola, G., Nikolaus, J., Tan, K.T., Nowak, C., Herrmann, A., Waldmann, H., Winter, R., et al. (2009). The lipid modifications of Ras that sense membrane environments and induce local enrichment. Angew. Chem. Int. Ed. *48*, 8784–8787.

Vogel, A., Reuther, G., Roark, M.B., Tan, K.T., Waldmann, H., Feller, S.E., and Huster, D. (2010). Backbone conformational flexibility of the lipid modified membrane anchor of the human N-Ras protein investigated by solid-state NMR and molecular dynamics simulation. Biochim. Biophys. Acta *1798*, 275–285.

Volkert, M., Uwai, K., Tebbe, A., Popkirova, B., Wagner, M., Kuhlmann, J., and Waldmann, H. (2003). Synthesis and biological activity of photoactivatable N-Ras peptides and proteins. J. Am. Chem. Soc. *125*, 12749–12758.

Wang, T.Y., Leventis, R., and Silvius, J.R. (2001). Partitioning of lipidated peptide sequences into liquid-ordered lipid domains in model and biological membranes. Biochemistry *40*, 13031–13040.

Weise, K., Triola, G., Brunsveld, L., Waldmann, H., and Winter, R. (2009). Influence of the lipidation motif on the partitioning and association of N-Ras in model membrane subdomains. J. Am. Chem. Soc. *131*, 1557–1564.

Weise, K., Kapoor, S., Denter, C., Nikolaus, J., Opitz, N., Koch, S., Triola, G., Herrmann, A., Waldmann H., and Winter, R. (2011). Membrane-mediated induction and sorting of K-Ras microdomain signaling platforms. J. Am. Chem. Soc. *133*, 880–887.

Wittinghofer, A. and Waldmann H. (2000). Ras – A molecular switch involved in tumor formation. Angew. Chem. Int. Ed. *39*, 4192–4214.

Zacharias, D.A., Violin, J.D., Newton, A.C., and Tsien, R.Y. (2002). Partitioning of lipid-modified monomeric GFPs into membrane microdomains of live cells. Science *296*, 913–916.